

# Metallic wave-impedance matching layers for broadband terahertz optical systems

Josef Kröll<sup>1</sup>, Juraj Darmo<sup>1</sup>, and Karl Unterrainer<sup>1,2</sup>

<sup>1</sup> Photonics Institute, Vienna University of Technology, Vienna, A-1040 Austria

<sup>2</sup> Centre for Nano- and Microstructures, Vienna University of Technology, Vienna, A-1040 Austria

[juraj.darmo@tuwien.ac.at](mailto:juraj.darmo@tuwien.ac.at)

**Abstract:** We examine the potential of ultra-thin metallic layers for broadband wave-impedance matching in the terahertz frequency range. The metallic layer is modeled using Fresnel formulae for stratified optical medium. Experimental data for chromium and indium-tin-oxide layers, measured using time-domain terahertz spectroscopy over the frequency range 0.4 – 4.5 THz, are compared with theoretical results.

©2007 Optical Society of America

OCIS codes: (160.3900) Metals; (310.1620) Coatings

---

## References and links

1. D. M. Mittleman, *Sensing with Terahertz radiation* (Cambridge Press, Cambridge, 2003) and references therein.
  2. M. Born and E. Wolf, *Principles of Optics*, 7<sup>th</sup> edition (Cambridge Press, Cambridge, 1999), Section 1.6.4, pp. 64.
  3. M. Born and E. Wolf, *Principles of Optics*, 7<sup>th</sup> edition (Cambridge Press, Cambridge, 1999), Section 14.4 pp.752.
  4. B. Carli, "Reflectivity of metallic films in the infrared," J. Opt. Soc. Am. **67**, 908-909 (1977).
  5. B. P. Gorshunov, G. V. Kozlov, A. A. Volkov, S. P. Lebedev, I. V. Fedorov, A. R. Prokhorov, I. V. Makhov, J. Schuetzmann, and K. F. Renk, "Measurement of electrodynamic parameters of superconducting films in the far-infrared and submillimeter frequency ranges," Int. J. Infrared Millimeter Waves **14**, 683-702 (1993).
  6. M. Dressel and G. Gruener, *Electrodynamics of Solid* (Cambridge Press, Cambridge, 2002), Chap. 5, pp. 92-135.
  7. E. D. Palik, *Handbook of Optical Constants of Solids* (Academic Press, New York, 1985).
  8. M. A. Ordal, J. J. Long, R. J. Bell, S. R. Bell, R. R. Bell, R. W. Alexander, and C. A. Ward, "Optical properties of the metals Al, Co, Cu, Au, Fe, Pb, Ni, Pd, Pt, Ag, Ti, and W in the infrared and far infrared," Appl. Opt. **22**, 1099-1119 (1983).
  9. M. A. Ordal, R. J. Bell, R. W. Alexander, Jr., L. L. Long, and M. R. Querry, "Optical properties of fourteen metals in the infrared and far infrared: Al, Co, Cu, Au, Pb, Mo, Ni, Pd, Pt, Ag, Ti, V, and W," Appl. Opt. **24**, 4493-4499 (1985).
  10. T. Bauer, J. S. Kolb, T. Löffler, E. Mohler, H. G. Roskos, and U. C. Pernisz, "Indium-tin-oxide-coated glass as dichroic mirror for far-infrared electromagnetic radiation," J. Appl. Phys. **92**, 2210-2212 (2002).
  11. Q. Wu, M. Litz, and X.-C. Zhang, "Broadband detection capability of ZnTe electro-optic field detectors," Appl. Phys. Lett. **68**, 2924-2926 (1996).
  12. Q. Wu and X.-C. Zhang, "7 THz broadband GaP electro-optic sensor," Appl. Phys. Lett. **70**, 1784-1786 (1997).
  13. J. Kröll, J. Darmo, and K. Unterrainer, "High-performance terahertz electro-optic detector," Electron. Lett. **40**, 763-764 (2004).
  14. P. R. Griffiths and J. A. DeHaseth, *Fourier transform infrared spectroscopy* (Wiley, New York, 1986).
-

## 1. Introduction

In recent years developments in terahertz technology have established time-domain terahertz spectroscopy (THz-TDS) as an important state-of-the-art tool in physics, chemistry, and even medical applications [1]. The unique, otherwise hidden, features and characteristics of many materials become observable in the terahertz frequency range. The inherently large bandwidth of THz-TDS systems requires that equally broadband optical components are available to manipulate the terahertz beam. Here, efficient wave-impedance matching layers are needed to minimize the reflections of free-space propagating THz waves from refractive optic elements and beam splitters used in the THz beam path. Since the standard  $\lambda_0/4$  dielectric antireflection layer is not suitable for THz systems due to its inherently small bandwidth [2], we examine the potential of semi-metallic and metallic films to serve as effective antireflection coatings for broadband THz signals.

The optical properties and performance of thin metallic films in the far-infrared frequency region have already been studied theoretically and experimentally [3,4]. It has been shown that a free-standing metallic mirror with a reflectivity varying from zero to almost one can be built due to the finite value of the conductivity of a metallic film [4]. A behavior related to this fact, the disappearance of Fabry-Perot resonances probed by far-infrared continuous waves, was reported by Gorshunov *et al.* for superconducting NbN film [5] and by Dressel for VO<sub>2</sub> layers [6] deposited on a sapphire substrate. In this contribution, we show theoretically and demonstrate experimentally that ultra-thin metallic films work as efficient wave-impedance matching layers in the terahertz and mid-infrared frequency regions.

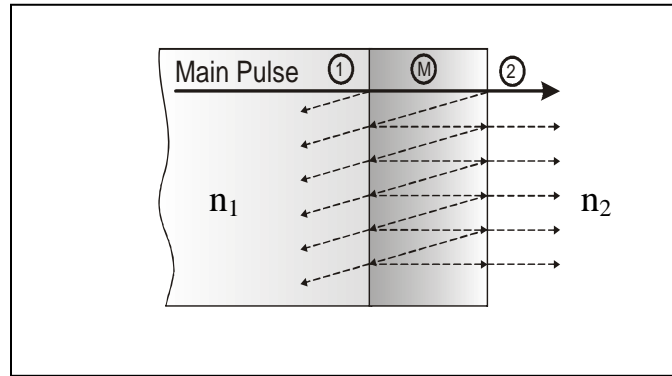


Fig. 1. Schematic of an optical system consisting of an optically thick material 1/thin metal layer (M)/optical material 2.

## 2. Model of optical wave-impedance matching layer

We examine the case when a sub-10 nm metallic film is placed at the interface between two different optical materials with the complex refractive indices  $n_1$  and  $n_2$  (Fig. 1). The metallic layer thickness is chosen such that the penetration depth (known as skin depth) of the electromagnetic radiation is larger than the layer thickness. In this instance the reflection and transmission of electromagnetic radiation can be described using a standard model [3]. The metallic layer is thus considered an ordinary optical layer, whose frequency response is described by the Drude model [6]. The electric field  $E_R$  of the reflected radiation is then given by

$$E_R = E_I \cdot \left( \frac{r_{1M} + r_{M2} \cdot t_M^2}{1 + r_{1M} \cdot r_{M2} \cdot t_M^2} \right), \quad (1)$$

where  $E_I$  is the electric field of the incident radiation;  $r_{xy}$  and  $t_{xy}$  are the Fresnel reflection and transmission coefficients (in general complex values) for an interface consisting of materials  $x$  and  $y$ ;  $t_M$  is the transmission coefficient through the metallic layer, and includes a phase shift as well as the attenuation losses of the electromagnetic wave as it propagates through the metal, i.e.  $t_M = \exp[i \cdot d \cdot 2\pi/\lambda_0 \cdot (n + i \cdot k) \cdot \cos \theta_M]$  where  $n$  and  $k$  are the real and imaginary parts of the metal's complex refractive index;  $d$  is the effective metal layer thickness; and finally  $\theta_M$  is the angle satisfying the Snell's law of refraction,  $n_1 \cdot \sin \theta_1 = (n + i \cdot k) \cdot \sin \theta_M = n_2 \cdot \sin \theta_2$ . The reflection at the interface is suppressed when the nominator of Eq. (1) is equal to zero, i.e.

$$r_{1M} + r_{M2} \cdot \exp[i \cdot d \cdot 4\pi/\lambda_0 \cdot (n + i \cdot k) \cdot \cos \theta_M] = 0. \quad (2)$$

Several possible solutions of Eq. (2) exist. Assuming a lossless dielectric layer ( $k = 0$ ), with  $r_{1M} = r_{M2}$  the ideal refractive index of the matching dielectric layer is given by  $n = \sqrt{n_1 \cdot n_2}$ . In this instance dielectric layer thickness  $d$  should be set to  $d = (2m+1) \cdot \lambda_0 / (4 \cdot n) \cdot \cos \theta_M$  ( $m = 0, 1, 2, \dots$ ) as is discussed in Ref. [2].

An alternative non-trivial solution exists that satisfies Eq. (2) for an absorptive layer (non-zero  $k$ ). Assuming normal incidence, i.e.  $\theta_M = 0$ , the following conditions for amplitude and phase arguments of the reflections coefficients hold

$$|r_{1M}| = |r_{M2}| \cdot \exp\left(-\frac{4\pi}{\lambda_0} \cdot d \cdot k\right) \quad (3a)$$

$$\exp(i \cdot \phi_{1M}) = -\exp\left(i \cdot \left(\phi_{M2} + \frac{4\pi}{\lambda_0} \cdot d \cdot n\right)\right), \quad (3b)$$

where  $\phi_{1M}$  and  $\phi_{M2}$  are the phases of reflection coefficients  $r_{1M}$  and  $r_{M2}$ . For an ultra-thin conductive layer ( $d \sim 1 - 10$  nm) at terahertz frequencies ( $\lambda_0 \sim 30 - 3000$   $\mu\text{m}$  or  $\nu = 0.1 - 10$  THz) we can easily satisfy  $(d \cdot k / \lambda_0)^2 \ll 1$  and  $(d \cdot n / \lambda_0)^2 \ll 1$ , hence Eq. (3a) can be Taylor expanded to the first order of Exp argument to give

$$|r_{1M}| = |r_{M2}| \cdot \left(1 - \frac{4\pi}{\lambda_0} \cdot d \cdot k\right), \quad (4a)$$

and phase arguments in (3b) have to satisfy an equation

$$\phi_{1M} - \phi_{M2} - \frac{4\pi}{\lambda_0} \cdot d \cdot n = (2m+1) \cdot \pi \quad \text{for } m = 0, 1, 2, \dots \quad (4b)$$

Equation (4a) indicates that  $r_{1M}$  has to be slightly smaller than  $r_{M2}$ . This occurs when  $n_1 > n_2$ , i.e. for electromagnetic waves propagating from the optically denser material to the less dense one. For a particular metal, with given optical parameters, the difference in the reflections from the  $n_1/\text{metal}$  and  $\text{metal}/n_2$  interfaces can be compensated for by varying the thickness of the metal film according to Eqs. (4a) and (4b). In Fig. 2(a) the total reflection coefficient, (calculated for 1.5 THz using our model) is plotted as a function of the conductance of the metal film for different refractive index ratios  $n_1/n_2$ . For these calculations we have chosen an arbitrary metal satisfying the Hagen-Rubens regime [6] at 1.5 THz, i.e. the real part of the metal conductivity  $\sigma_r$  is frequency independent and  $\sigma_r \gg \sigma_i$ . The electric field of the reflected radiation changes amplitude and phase shifts by  $\pi$  as the sheet conductance and thus the thickness of the metallic layer increases. The position of the zero total reflection crossing

point ( $E_R=0$ ) depends on the mismatch between the optical materials. Generally, if this mismatch is large, the conductance of the matching layer must also be made large to ensure proper matching between the materials.

One drawback of metallic wave-impedance matching layers is the energy loss due to absorption in the metal. This loss scales with the wave-impedance difference between optical materials. If the wave impedance difference between the optical materials is large then the matching conditions are more severe, requiring that a thicker metallic layer, with a correspondingly higher sheet conductance [see Fig. 2(b)], has to be used. This in turn leads to the larger absorption losses. This is illustrated clearly in Fig. 2(c) where the absorption loss in the impedance matching metallic layer is plotted as a function of the refractive index mismatch. We note that these losses are about twice the reflection losses incurred at the dielectric interface  $n_1/n_2$  without an impedance matching layer.

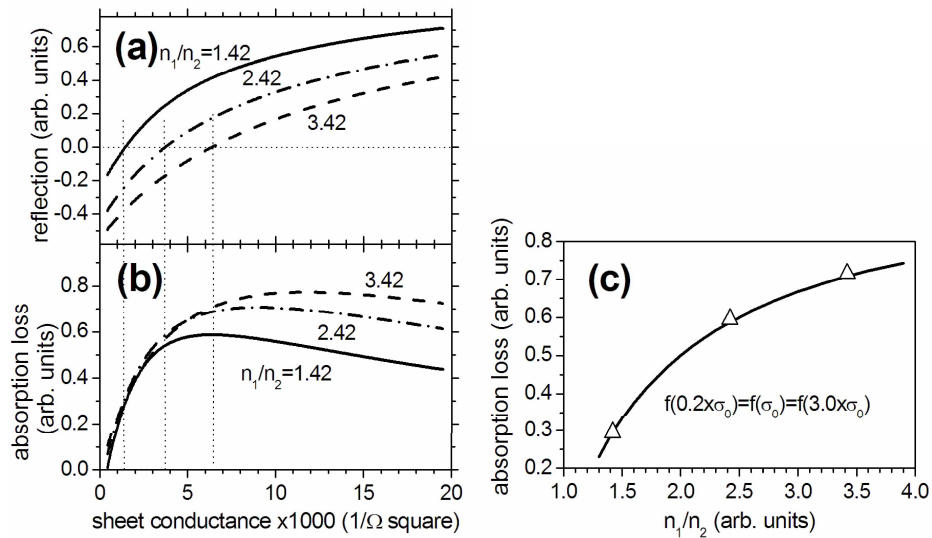


Fig. 2. Dependence of (a) the reflection and (b) absorption losses of 1.5 THz radiation on the metallic layer sheet conductance for the optical system depicted in Fig. 1 for different refractive index ratios  $n_1/n_2$ . (c) Absorption losses at 1.5 THz in the metallic wave-impedance matching layer as a function of the refractive index mismatch (given in ratio  $n_1/n_2$ ). The losses are independent from the metal conductivity ( $\sigma_0$  – reference metal conductivity).

The main advantage that the metallic wave-impedance matching film has over the standard  $\lambda_0/4$  dielectric antireflection layers is its superior frequency performance. The phase shift in the case of the  $\lambda_0/4$  dielectric antireflection layer scales as  $\lambda_0^{-1}$ . Since the metal plasma frequency is generally high ( $\lambda_{\text{plasma}} \sim 0.1 - 10 \mu\text{m}$ ) [7-9], at THz frequencies we are in fact in the Hagen-Rubens regime [6] which implies  $n, k \sim \lambda_0^{1/2}$ . That means that the frequency dependence of matching performance of the metallic layer is by principle weaker in comparison to the standard  $\lambda_0/4$  dielectric antireflection layer and the bandwidth is in fact  $\sqrt{2}$  wider (see Fig. 3). The bandwidth in this case is defined as a frequency range where the total reflection coefficient is  $< 0.01$ .

The bandwidth of the metallic wave-impedance matching layer can be further increased if we assume that the left-hand side of Eq. (2) is equal to a small number, e.g.  $10^{-2}$ , instead of the somewhat stricter requirement that it be equal to zero. In this case the reflected power is four orders of magnitude smaller than the transmitted one which is satisfactory for most applications. Due to the magnitude of optical parameters ( $n, k \gg 1$ ) of metal in the Hagen-

Rubens regime the phases of the reflection coefficients  $r_{1M}$  and  $r_{M2}$  are very similar but of opposite sign. This situation is completely different from the case of the standard  $\lambda_0/4$  dielectric antireflection layers, in which the phase shift of individual reflections is zero. Therefore, the additional phase shift acquired by wave traveling in the metal layer, and necessary to achieve  $\pi$  phase difference of the waves reflected at individual interfaces  $n_1/\text{metal}$  and  $\text{metal}/n_2$  is very small, usually several milliradians in the contrast to the standard antireflection layer. The frequency dependent phase argument in Eq. (4b) holds  $(4 \cdot d \cdot n / \lambda_0) \ll 1$  in the case of thin metallic layer, while for the standard  $\lambda_0/4$  dielectric antireflection layer it is of  $(4 \cdot d \cdot n / \lambda_0) \approx 1$ . In practice this means that tolerating a small non-zero reflection coefficient allows the use of a metallic wave-impedance matching layer over frequency range orders of magnitude wider than the standard  $\lambda_0/4$  dielectric antireflection layer. The frequency dependence of the reflection coefficient shown in Fig. 3 (model details are in the figure caption) clearly demonstrates this fact. We call an ultra-thin metallic layer that reduced significantly the reflection of the electromagnetic waves at interface of two optically different materials as Metallic AntiReflection Coating (MARC).

At somewhat higher frequencies (in the relaxation regime of the metal response)  $k$  scales as  $\lambda_0$  and  $n$  as  $\lambda_0^2$ . Therefore, the term in the parenthesis on right-hand side of Eq. (4a) is frequency independent in the relaxation regime. The phase of the reflection changes [Eq. (4b)] stays frequency dependent, but if  $(4 \cdot d \cdot n / \lambda_0) \ll 1$  still hold and the metallic layer could be used as a broadband antireflection coating also at frequencies within the relaxation regime of the metal response.

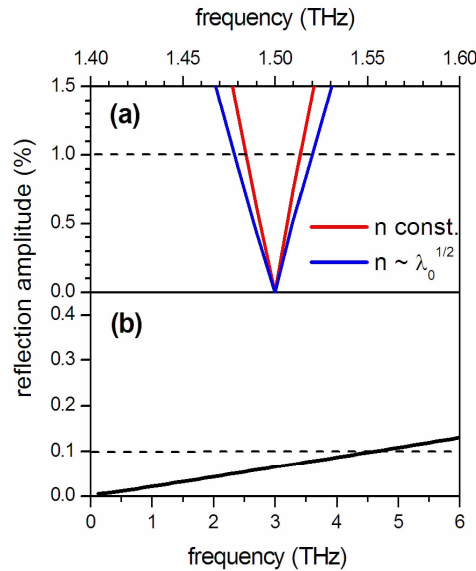


Fig. 3. Amplitude of the reflection coefficient at the interface GaAs ( $n_1=3.415$ ) and air as a function of frequency with (a) dielectric  $\lambda_0/4$  antireflection layer and (b) metallic antireflection layer (metal conductivity  $\sigma_0$  of  $7.87 \times 10^6$  S/cm, thickness 16.3 nm). Antireflection layers were optimized for the frequency of 1.5 THz. In that case the total reflection coefficient is less than 0.1% in the frequency range 0.1 – 4.5 THz, while the reflection coefficient stays below 1% in the frequency range as narrow as 30 GHz for the dielectric antireflection layer. This bandwidth can be increased for the hypothetical dielectric material for which  $n$  scales as  $\lambda_0^{1/2}$  (blue line).

### 3. Experimental results

The effect of an ultra-thin metallic layer on the reflection coefficient at an interface of two different optical materials was studied for two different material systems: First, a series of the highly resistive (resistivity  $> 3000 \Omega\text{cm}$ ) silicon plates were coated on one side with a chromium film with thicknesses ranging from 2 to 20 nm. The high resistive silicon is used because at THz frequencies it is transparent and has negligible dispersion. Chromium was chosen due to its excellent coating capability, allowing the thickness and the sheet resistance to be accurately controlled. The second chosen material system is highly resistive GaAs coated with indium-tin-oxide (ITO). Undoped GaAs exhibits low absorption and dispersion at THz frequencies. Indium-tin-oxide is a material with a metal-like conductivity, but is transparent in the visible and near-infrared wavelength unlike the most metals. Recently, ITO was used for dichroic near-infrared/THz mirrors [10].

The THz performance of the chromium and ITO layers was measured using a transmission THz-TDS system with a photo-conductive gallium-arsenide emitter and a 300- $\mu\text{m}$  thick gallium-phosphide electro-optic electric field sensor. This THz setup enables spectral sensing range 0.1 to 7 THz with an  $\text{SNR} > 1$ .

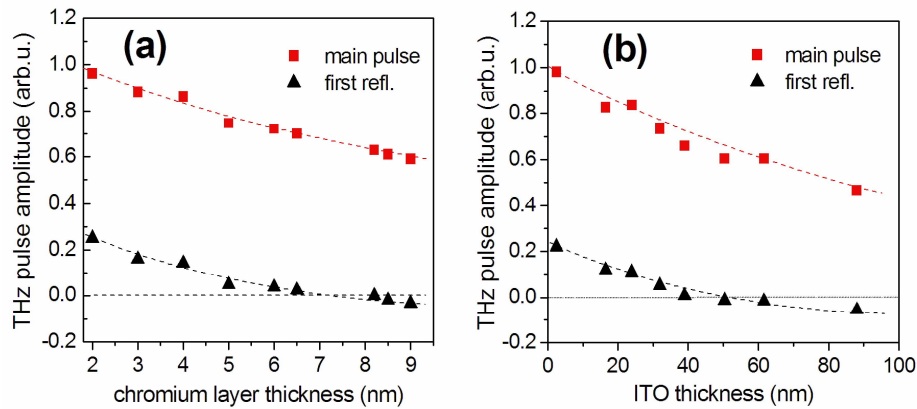


Fig. 4. Amplitude of the main and the first reflected THz pulses transmitted through (a) 400  $\mu\text{m}$  thick silicon plate with a chromium film; (b) 510  $\mu\text{m}$  thick gallium-arsenide with an indium-tin-oxide film. (lines – simulation using the theory [6]).

The time-domain signal measured with this type of experimental setup typically consists of several THz pulses; the main pulse transmitted through sample and followed by a train of successive pulses of decreasing amplitude. Each of these successive pulses is delayed from main pulse by a multiple of the round-trip time within the sample. In Fig. 4(a) the amplitudes of the main and the first reflected THz pulses are shown. Amplitudes of both pulses are normalized with respect to the amplitude of the main THz pulse transmitted through the uncoated silicon plate. As expected, the amplitude of the main transmitted THz pulse decreases as thickness of the chromium and ITO film increases due to absorption losses in the metal film. The amplitude of the reflected THz pulse also decreases, goes through zero, and after a change of polarity it raises again in coherence with the theoretical predictions shown in Fig. 2. For a chromium layer thickness of about 8.3 nm the reflection of THz pulse from the system silicon/chromium/air vanishes. The same behavior was observed for the material system GaAs/indium-tin-oxide. Since the conductivity of the ITO is smaller than that of chromium, the optimal thickness of ITO for the reflection cancellation is relatively large  $\sim 44$  nm [Fig. 4(b)].

We have compared our experimental data with the results predicted from the model and we found good agreement between them. We attribute any recognized differences to the limited validity of the Drude model [6, 8] at the THz frequencies, especially when the input model parameters (scattering rate, carrier density at Fermi surface) that we used, were obtained from measurements of DC conductivity of the chromium and ITO layers. In addition, deviation of the optical parameters of a metal from the Drude model is usually observed for the transition metals like chromium [8]. Therefore, the optimal thickness of metal film for a given sample material almost always has to be estimated experimentally.

The measured THz signal, transmitted through both a coated and uncoated silicon plate, is presented in Fig. 5(a) (see caption for details). For the uncoated sample (red line) a secondary pulse can be seen approximately 9 ps after the initial pulse. However when the silicon plate is coated with a 8.3 nm of chromium, which corresponds to the optimized thickness, the secondary pulse is completely suppressed (black line).

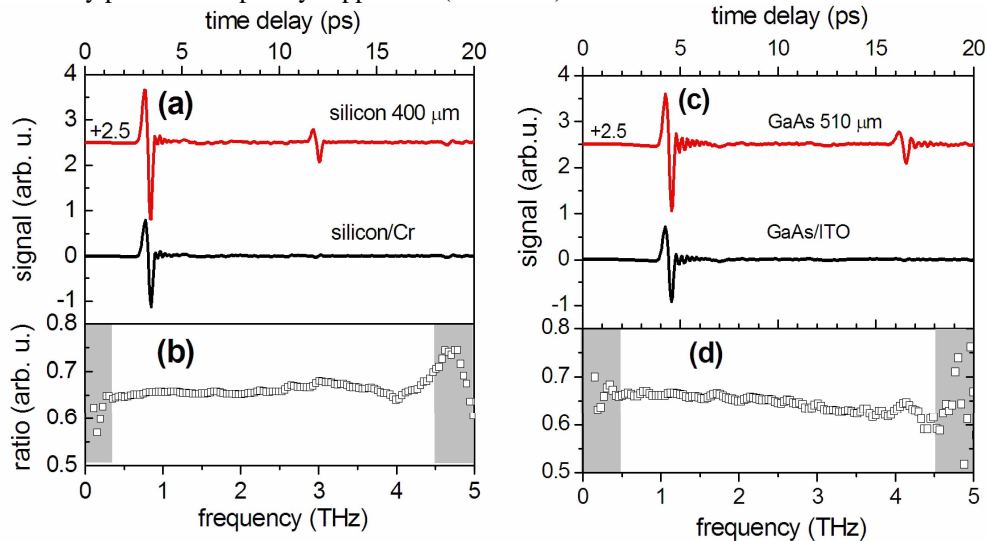


Fig. 5. Transmitted THz-TDS signal for (a) a 400 $\mu\text{m}$  thick silicon plate both uncoated (red line) and Cr-coated (black line) and (c) a highly resistive uncoated (red) GaAs wafer and its ITO-coated (black) counterpart. Spectral ratio of transmitted THz pulses through the silicon (b) and GaAs (d) with optimized antireflection coatings.

Similarly in Fig. 5(c) we present the measured THz signal for a coated (44 nm thick ITO layer) and uncoated GaAs sample. By comparing the coated (red) and uncoated (black) traces in Fig. 5(c) it is evident that the second reflected pulse has also disappeared. These experimental results clearly demonstrate the effectiveness of our wave-impedance matching technique.

In Figs. 5(b) and 5(d) we demonstrate the effect of our coatings on the spectral characteristics of the THz signal. The spectral response for the coated sample is normalized with respect to the spectral response for the uncoated sample and presented as a spectral “ratio”. This spectral ratio stays approximately constant over a 4 THz range (0.4 to 4.5 THz) proving frequency independent behavior of the metallic coating. We note that analysis of measurement data at frequencies below 0.4 and above 4.5 THz is limited by the SNR of data.

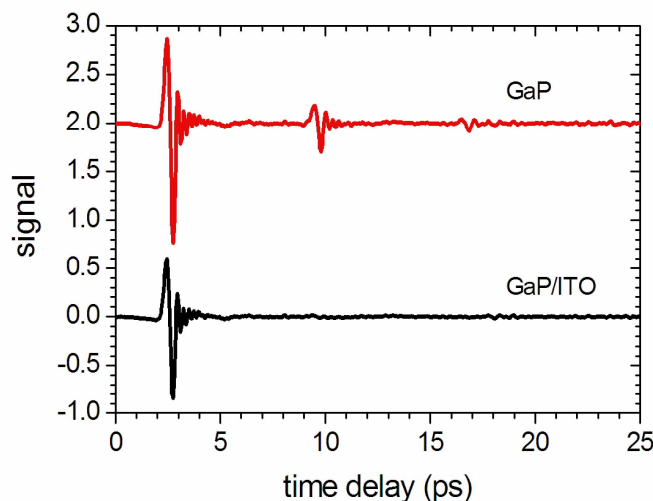


Fig. 6. Electric field of THz transient sensed with a 300 $\mu$ m thick uncoated gallium phosphide electro-optic crystal and gallium phosphide crystal with ITO based MARC. In the uncoated crystal THz pulse several times bounces leading to ~7 ps delayed gradually attenuated pulses.

The effectiveness of the ITO based MARC is also demonstrated for an electro-optic GaP crystal. This non-linear optical material can be used as a broadband detector of the coherent terahertz radiation by exploiting the Pockel effect [11, 12]. To ensure operation over a large bandwidth, the GaP crystal has to be thin [12]. This however reduces the quality of the time-domain signal due to reflections of THz radiation from the crystal/air interfaces. Recently, we proposed a solution to this problem using an ultra-thin chromium film [13]. One major drawback to this solution is the loss of about 45% of the near-infrared ( $\lambda=800$  nm) probe power due to the chromium film. By replacing the chromium film with an ITO based MARC this 45% loss can be avoided, improving the detector performance. In Fig. 6 the time-domain response of the THz pulse detected at 300  $\mu$ m thick GaP, with and without an applied ITO based MARC, is shown.

Finally, we demonstrate how the MARC can be used effectively for Fourier transform infrared spectroscopy (FTIR) in the mid infrared frequency range. The spectral characteristics of 370  $\mu$ m thick GaAs wafer used as a beam splitter were estimated over the range 5 – 20  $\mu$ m using FTIR. The measured spectrum, shown in Fig. 7, is strongly modulated by Fabry-Perot oscillations that arise due to interferences within the wafer. In the uncoated sample (red line) the absorption line of CO<sub>2</sub> molecule at 14.978  $\mu$ m is barely visible, inhibiting standard quantitative analysis of the CO<sub>2</sub> concentration [14]. If the same GaAs beam splitter is now coated with a MARC, the overall signal strength drops, but the Fabry-Perot oscillations are completely removed and good quality spectrum is obtained.



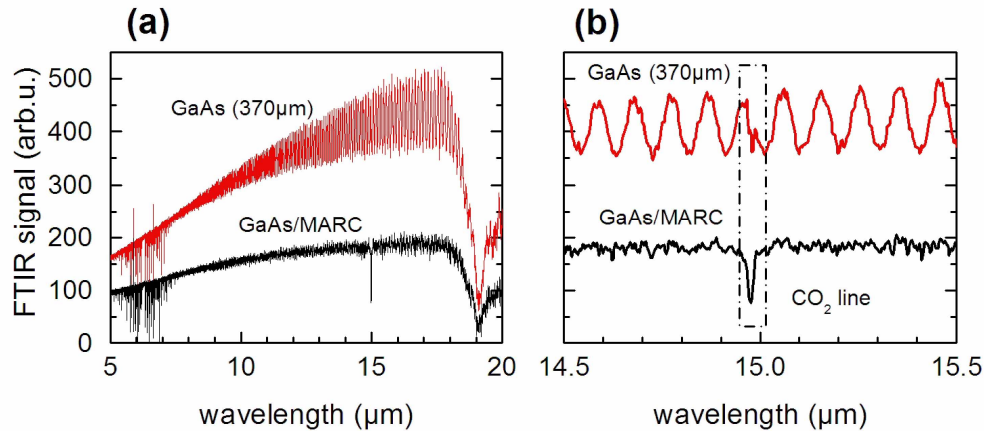


Fig. 7. (a). Spectra obtained by a Fourier transform infrared spectroscopic system with GaAs beam splitter without and with metallic antireflection layer; (b) Details of the spectra from the left panel. The CO<sub>2</sub> absorption line at 667.6 cm<sup>-1</sup> (14.978 μm) is well resolved for when the antireflection layer is applied to the beam splitter.

#### 4. Summary

In summary, we have shown that the amplitude and phase of few-cycle THz pulses reflected at dielectric interfaces covered with a metal film can be efficiently minimized by controlling the film thickness. We modeled this behavior using Fresnel formulae applied to the stratified medium. We demonstrated experimentally that ultra-thin chromium and ITO films can be used as an efficient broadband antireflection coating for optical components in the terahertz frequency range.

#### Acknowledgments

The authors acknowledge financial support from the European commission (IST-511415 “Teranova”), the Austrian “Fonds zur Förderung der Wissenschaftlichen Forschung” (project SFB-ADLIS) and the “Gesellschaft für Mikroelektronik”.